# An anticipatory approach to optimal experimental design for model discrimination

Brecht M.R. Donckels [a,b,*], Dirk J.W. De Pauw [b], Bernard De Baets [b], Jo Maertens [a], Peter A. Vanrolleghem [c]

[a] BIOMATH, Department of Applied Mathematics, Biometrics and Process Control, Ghent University, Coupure links 653, B-9000 Ghent, Belgium
[b] KERMIT, Department of Applied Mathematics, Biometrics and Process Control, Ghent University, Coupure links 653, B-9000 Ghent, Belgium
[c] modelEAU, Département de génie civil, Pavillon Pouliot, Université Laval, Québec, QC, Canada G1K 7P4

## ARTICLE INFO

## ABSTRACT

The problem of model discrimination arises when several models are proposed to describe one and the same process. To identify the best model from the set of rival models, it may be necessary to collect new information about the process, and thus additional experiments have to be performed. This paper deals with the experimental design methodologies that are used to find the experimental conditions that allow to discriminate among rival models with the least experimental effort. For this, the expected experimental results should be predicted differently by the rival models, and the uncertainty on the measurements and on the model predictions should not be too large. These aspects were included in the approach developed by Buzzi-Ferraris and co-workers [G. Buzzi-Ferraris, P. Forzatti, G. Emig, H. Hofmann, Sequential experimental design procedure for model discrimination in the case of multiple responses. Chemical Engineering Science (1) (1984) 81–85], but in their approach the uncertainties are estimated from the information content of the already performed experiments. This work presents a modification of the Buzzi-Ferraris approach in which the expected information content of the newly designed experiment is considered, even before the experiment is performed (anticipatory design). In this way, a better estimate of the uncertainties is achieved, and an experiment with an increased discriminatory potential is obtained. The approaches were illustrated and compared by applying them to a case study in which two rival models are proposed to describe the *in vitro* kinetics of an enzyme.

© 2008 Elsevier B.V. All rights reserved.

## 1. Introduction

Mathematical models are useful tools for engineers. Next to increasing insight in often complex processes, mathematical models are used in process design, optimization and control. How one obtains such models will not be discussed here. However, it is important to realize that the lack of insight in the modeled system may result in the proposal of several rival models. Obviously, one is especially interested in the model that describes the system under study in the best way. To identify this model from a set of rival models, it may be necessary to collect new information about the system, and thus additional experiments have to be performed.

A general methodology to discriminate among rival models is given in Fig. 1. It basically consists of four steps that are performed in an iterative manner until a stopping criterion is met. The rival models and the preliminary experimental data are used in a first step, in which the parameters of the rival models are estimated. A

second step involves model adequacy testing, performed to find out which models are able to describe the data in a reasonable manner and which ones do not. Models that pass this test are used in a third step, where an optimal discriminatory experiment is designed. This experiment is then performed in a fourth and last step, after which the loop is closed by re-estimating the parameters of all rival models using all data available at that time. This iterative procedure continues until the best model is identified. Of course, when all models appear to be inadequate, new models have to be proposed.

The methodologies to design experiments that allow to discriminate among rival models, often referred to as optimal experimental design for model discrimination (OED/MD) [10–14,17,41,43] or optimal experimental design for (model) structure characterization (OED/SC) [9,44–46], will be the focus of this paper. The main contribution of this work is a modification of an existing methodology [13] that has been successfully used by others [10,11,13,26,41] to design an optimal discriminatory experiment. These methods will be described in Section 2, together with some other theoretical aspects that are indirectly related. Section 3 describes and discusses the results of a case study in which the different methodologies were applied and compared. Finally, some concluding remarks are presented in the last section.

* Corresponding author. BIOMATH, Department of Applied Mathematics, Biometrics and Process Control, Ghent University, Coupure links 653, B-9000 Ghent, Belgium.
*E-mail address:* brecht.donckels@biomath.ugent.be (B.M.R. Donckels).

## 2. Methods

### 2.1. Mathematical model representation

In what follows, general deterministic models in the form of a set of (possibly mixed) differential and algebraic equations are considered, using the following notations:

$$\dot{\boldsymbol{x}}(t) = \boldsymbol{f}(\boldsymbol{x}(t), \boldsymbol{u}(t), \boldsymbol{\theta}, t); \quad \boldsymbol{x}(t_0) = \boldsymbol{x}_0 \tag{1}$$

$$\hat{\boldsymbol{y}}(t) = \boldsymbol{g}(\boldsymbol{x}(t)) \tag{2}$$

where $\boldsymbol{x}(t)$ is an $n_s$-dimensional vector of time-dependent state variables, $\boldsymbol{u}(t)$ is an $n_u$-dimensional vector of time-varying inputs to the process, $\boldsymbol{\theta}$ is an $n_p$-dimensional vector of model parameters taken from a continuous, realizable set $\boldsymbol{\Theta}$, and $\hat{\boldsymbol{y}}(t)$ is an $n_m$-dimensional vector of measured response variables that are function of the state variables, $\boldsymbol{x}(t)$. An experiment will be denoted as $\boldsymbol{\xi}$, and is determined by the experimental degrees of freedom which can for instance be measurement times, initial conditions and time-varying or constant process inputs.

### 2.2. Parameter estimation

The values of the model parameters, which by definition do not change during the course of the simulation, have to be determined from experimental data. This process is called parameter estimation, and typically consists of minimizing the weighted sum of squared errors (WSSE) functional by optimal choice of the parameters $\boldsymbol{\theta}$. The WSSE is calculated as follows

$$\text{WSSE}\left(\hat{\boldsymbol{\theta}}\right) = \sum_{k=1}^{n_e} \sum_{l=1}^{n_{sp_k}} \Delta\hat{\boldsymbol{y}}\left(\boldsymbol{\xi}_k, \hat{\boldsymbol{\theta}}, t_l\right)' \cdot \mathbf{Q} \cdot \Delta\hat{\boldsymbol{y}}\left(\boldsymbol{\xi}_k, \hat{\boldsymbol{\theta}}, t_l\right), \tag{3}$$

where

$$\Delta\hat{\boldsymbol{y}}\left(\boldsymbol{\xi}_k, \hat{\boldsymbol{\theta}}, t_l\right) = \boldsymbol{y}(\boldsymbol{\xi}_k, t_l) - \hat{\boldsymbol{y}}\left(\boldsymbol{\xi}_k, \hat{\boldsymbol{\theta}}, t_l\right) \tag{4}$$

represents the difference between the vector of the $n_m$ measured response variables and the model predictions at time $t_l$ ($l = 1,\dots,n_{sp_k}$) of experiment $\boldsymbol{\xi}_k$ ($k = 1,\dots,n_e$). Further, $n_e$ represents the number of experiments from which data is used for estimating the parameters, $n_{sp_k}$ represents the number of samples in experiment $\boldsymbol{\xi}_k$, and $\mathbf{Q}$ is an $n_m$-dimensional matrix of user-supplied weighing coefficients. Typically, $\mathbf{Q}$ is chosen as the inverse of the measurement error covariance matrix $\boldsymbol{\Sigma}$ [29,38,46]. In this way, the measurement uncertainty is incorporated in the WSSE.
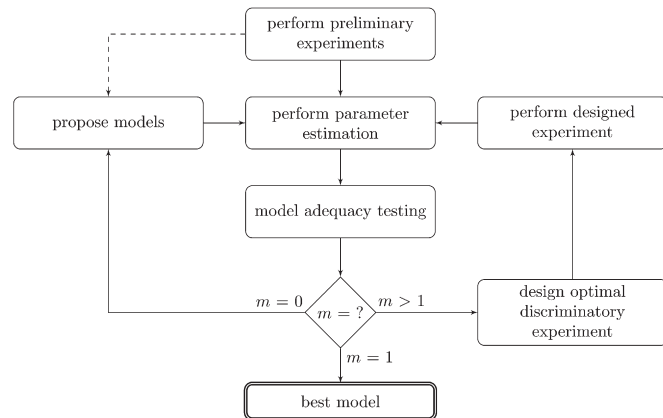
**Fig. 1.** General methodology to discriminate among $m$ rival models (adapted from [17] and [41]).

### 2.3. Parameter estimation uncertainty

Since the parameters are estimated from noise-corrupted experimental data, the resulting parameter estimates will be uncertain to some extent. This section explains the approach followed in this work to quantify this uncertainty.

The parameter estimation error covariance matrix, denoted as $\boldsymbol{\Phi}$, represents the uncertainty on the parameter estimates. Obviously, the quality of these parameter estimates is determined by the information content of the experimental data from which they are determined. The latter can be quantified by means of the so-called Fisher information matrix (**FIM**), the inverse of which is often used as an approximation of the parameter estimation error covariance matrix [1,3,22,28,30,35,40,46,47]. The **FIM** is calculated as

$$\mathbf{FIM} = \sum_{k=1}^{n_e} \mathbf{FIM}(\boldsymbol{\xi}_k), \tag{5}$$

where

$$\mathbf{FIM}(\boldsymbol{\xi}_k) = \sum_{l=1}^{n_{sp_k}} \boldsymbol{S}_{\hat{\boldsymbol{\theta}}}^{\hat{\boldsymbol{y}}}(\boldsymbol{\xi}_k, t_l)' \cdot \boldsymbol{\Sigma}(\boldsymbol{\xi}_k, t_l)^{-1} \cdot \boldsymbol{S}_{\hat{\boldsymbol{\theta}}}^{\hat{\boldsymbol{y}}}(\boldsymbol{\xi}_k, t_l). \tag{6}$$

Here, $\boldsymbol{S}_{\hat{\boldsymbol{\theta}}}^{\hat{\boldsymbol{y}}}(\boldsymbol{\xi}_k, t_l)$ represents the $n_m \times n_p$-dimensional parameter sensitivity matrix associated with measurement time $t_l$ of experiment $\boldsymbol{\xi}_k$, and is calculated as

$$\boldsymbol{S}_{\hat{\boldsymbol{\theta}}}^{\hat{\boldsymbol{y}}}(\boldsymbol{\xi}_k, t_l) = \left.\frac{\partial\hat{\boldsymbol{y}}(\boldsymbol{\xi}_k, \boldsymbol{\theta}, t_l)}{\partial\boldsymbol{\theta}}\right|_{\hat{\boldsymbol{\theta}}}. \tag{7}$$

To calculate these parameter sensitivities, $n_m \times n_p$ additional ordinary differential equations are defined and solved together with the actual model. These equations are obtained by explicit calculation of the total differentials. For detailed information on this matter, the reader is referred to [27,34,43].

A closer look at Eq. (6), shows that the **FIM** is composed of two components, the parameter sensitivities ($\boldsymbol{S}_{\hat{\boldsymbol{\theta}}}^{\hat{\boldsymbol{y}}}$) and the measurement error covariance matrix ($\boldsymbol{\Sigma}$). The parameter sensitivity with respect to a certain state variable expresses how much that state variable will change when a parameter is slightly perturbed. A state variable that is highly sensitive to a certain parameter will therefore contain a lot of information about this parameter, while a variable that is insensitive to the parameter does not contribute to the information content for that parameter. The role of the measurement error covariance matrix in the calculation of the **FIM** is rather straightforward, since it is obvious that a measurement associated with a large measurement error will contribute less to the information content than a measurement with a small measurement error.

From the parameter estimation error covariance matrix, the $100 \cdot (1 - \alpha)$ percent confidence interval associated with parameter estimate $i$ can be calculated as [29]

$$\sqrt{\Phi(i, i)} \cdot t_{n-n_p}^{\alpha/2}, \tag{8}$$

where $n$ represents the total number of data points, $n_p$ represents the number of parameters that were estimated, and $t_{n-n_p}^{\alpha/2}$ represents the upper $\alpha/2$ quantile of Student's $t$ distribution for the given confidence level $\alpha$ and $n - n_p$ degrees of freedom.

### 2.4. Model prediction uncertainty

The uncertainty on the parameter estimates will propagate when simulating the model, and the model predictions will consequently be uncertain as well. Also in the case of model predictions, a covariance matrix is used to quantify the uncertainty. The model prediction error covariance matrix associated with time $t_l$ of experiment $\boldsymbol{\xi}_k$, denoted

as $\Omega(\boldsymbol{\xi}_k, t_l)$, is calculated by propagating the uncertainty on the parameter estimates, according to [38]

$$\Omega(\boldsymbol{\xi}_k, t_l) = \boldsymbol{S}_{\hat{\boldsymbol{\theta}}}^{\hat{\boldsymbol{y}}}(\boldsymbol{\xi}_k, t_l) \cdot \boldsymbol{\Phi} \cdot \boldsymbol{S}_{\hat{\boldsymbol{\theta}}}^{\hat{\boldsymbol{y}}}(\boldsymbol{\xi}_k, t_l)'. \tag{9}$$

The confidence intervals associated with the model predictions are calculated in a similar way as those of the parameter estimates (Eq. (8)) [38].

## 2.5. A note on the linear approximation of parameter and model prediction uncertainties

The common approaches to determine the parameter and model prediction uncertainties are based on linear propagations of uncertainties, and on the assumption of Gaussian white noise. Consequently, they should only be considered as approximate estimates, especially when working with non-linear models. Nevertheless, it is a common practice to use these approximations for experimental design purposes. When designing experiments to increase the accuracy of the parameter estimates, for instance, scalar functions of the **FIM** are maximized (for instance in [3,4,9,19,28,35,45–47]), and also the design of optimal discriminatory experiments often relies on linear approximations of the model prediction uncertainties (as discussed below).

Experimental designs based on these approximations can therefore be less informative than expected [8]. However, from a heuristic point of view, they are still very useful. Some interesting techniques have been described in literature [1,2,8,24,38,47] to achieve better approximations of the uncertainties for non-linear models, but these are computationally demanding. This currently makes them less suited [24] for optimal experimental design purposes.

## 2.6. Model adequacy testing

To test a model's adequacy, a lack-of-fit test, as outlined for instance in [14,17,18], can be used. This test is based on the property of the WSSE-functional being a sample from a $\chi^2$ distribution with $n - n_p$ degrees of freedom. However, this property only holds under two assumptions [18]: (i) the measurements are disturbed with random zero mean normally distributed noise with known (or a priori estimated) variance, and are not subject to systematic errors; and (ii) no model errors are present.

In this work, data is generated by adding noise to the simulation results of which the characteristics are known, so the first assumption is always valid. Consequently, when the WSSE is significantly larger than the expected value of the appropriate $\chi^2_{n - n_p}$ distribution, one can conclude that the model is not able to describe the experimental data in a reasonable manner and the model can thus be rejected.

## 2.7. Optimal experimental design for model discrimination

In general, optimal experimental design is an optimization problem, where the optimum of a well-defined objective function is sought by varying the experimental degrees of freedom. This can be formalized as follows

$$\boldsymbol{\xi}^{\star} = \arg\max_{\boldsymbol{\xi} \in \Xi} T(\boldsymbol{\xi}). \tag{10}$$

The experimental degrees of freedom, $\boldsymbol{\xi}$, are restricted by a number of constraints that define a set of possible experiments, denoted as $\Xi$. These constraints are determined by the experimental setup and are specified before the start of the experimental design exercise.

### 2.7.1. Objective functions for OED/MD

Suppose, for simplicity, that one has to design an experiment to discriminate between two rival models ($m = 2$). It is clear that the data expected from the designed experiment should be predicted differently by the two models to allow for model discrimination. Hunter and Reiner translated this heuristic into an objective function [23] given by

$$T_{ij}(\boldsymbol{\xi}) = \sum_{l=1}^{n_{sp}} \Delta \hat{\boldsymbol{y}}_{ij}\left(\boldsymbol{\xi}, \hat{\boldsymbol{\theta}}_i, \hat{\boldsymbol{\theta}}_j, t_l\right)' \cdot \Delta \hat{\boldsymbol{y}}_{ij}\left(\boldsymbol{\xi}, \hat{\boldsymbol{\theta}}_i, \hat{\boldsymbol{\theta}}_j, t_l\right), \tag{11}$$

where

$$\Delta \hat{\boldsymbol{y}}_{ij}\left(\boldsymbol{\xi}, \hat{\boldsymbol{\theta}}_i, \hat{\boldsymbol{\theta}}_j, t_l\right) = \hat{\boldsymbol{y}}_i\left(\boldsymbol{\xi}, \hat{\boldsymbol{\theta}}_i, t_l\right) - \hat{\boldsymbol{y}}_j\left(\boldsymbol{\xi}, \hat{\boldsymbol{\theta}}_j, t_l\right) \tag{12}$$

represents the difference between the $n_m$-dimensional vectors of the predicted outcomes of experiment $\boldsymbol{\xi}$ by model $i$ and model $j$ at time $t_l$, and $n_{sp}$ represents the number of samples. Note that this notation will be simplified to $\Delta \hat{\boldsymbol{y}}_{ij}(\boldsymbol{\xi}, t_l)$ in the following.

It is important to point out that this objective function does not take into account the uncertainty on the measurements, nor on the model predictions. However, it is important to do so, as illustrated in Fig. 2. The difference in the model predictions may be high for a particular subset of the experimental degrees of freedom, but when those experimental conditions result in a situation that is characterized by a high measurement error, discrimination may not be possible after all. This is the case for the group of measurements on the left in Fig. 2. A similar reasoning holds for the uncertainty on the model predictions. For instance, the group of measurements on the right (Fig. 2) has smaller measurement errors, and is located where the difference in the model predictions is significant. However, this region is not very interesting for model discrimination because of the large uncertainty on the model predictions. Model discrimination will be possible for the group of measurements in the middle, where both the measurement errors and the model prediction uncertainties are relatively small, and the difference in the model predictions is significant.

To incorporate the uncertainty on the measurements, a similar approach as the one used in Eq. (3) can be followed [21] resulting in

$$T_{ij}(\boldsymbol{\xi}) = \sum_{l=1}^{n_{sp}} \Delta \hat{\boldsymbol{y}}_{ij}(\boldsymbol{\xi}, t_l)' \cdot \boldsymbol{\Sigma}(\boldsymbol{\xi}, t_l)^{-1} \cdot \Delta \hat{\boldsymbol{y}}_{ij}(\boldsymbol{\xi}, t_l), \tag{13}$$

where $\boldsymbol{\Sigma}(\boldsymbol{\xi}, t_l)$ represents the measurement error covariance matrix at time $t_l$ of experiment $\boldsymbol{\xi}$.

The objective function proposed by Buzzi-Ferraris and co-workers [13] builds further on this and also incorporates the uncertainty on the model predictions. This is done by weighing the difference in the predicted outcomes of an experiment, denoted as $\Delta \hat{\boldsymbol{y}}_{ij}(\boldsymbol{\xi}, t_l)$, with the uncertainty associated with it. This uncertainty originates from
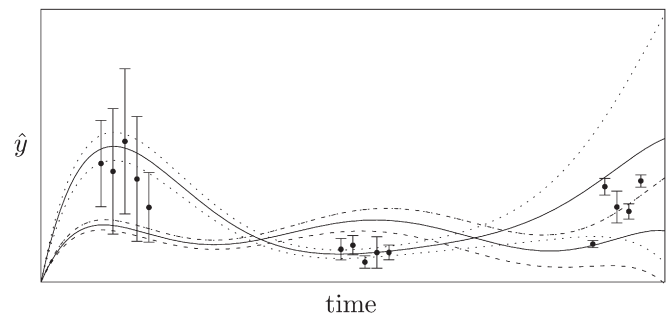


**Fig. 2.** Trajectories of two models (full lines) with their associated model prediction uncertainties (dotted/dashed lines), as well as a number of measurements (●) with their associated measurement uncertainty.

two sources. One has to consider the uncertainty on the model predictions as such (denoted as $\mathbf{\Omega}$), as well as the uncertainty on the measurements (denoted as $\mathbf{\Sigma}$). When $\mathbf{\Sigma}$ and $\mathbf{\Omega}$ are assumed to be independent, the uncertainty on the predicted outcome of an experiment can be estimated as $\mathbf{\Sigma}+\mathbf{\Omega}$. Although this assumption is not entirely valid, it is a reasonable one in this context because the objective function is used as a heuristic. Now, under a similar assumption, the uncertainty on the difference between the predicted outcomes of an experiment by model $i$ and $j$, denoted as $\mathbf{\Psi}_{ij}$, is given by

$$\begin{aligned}\mathbf{\Psi}_{ij} &= \mathbf{\Sigma} + \mathbf{\Omega}_i + \mathbf{\Sigma} + \mathbf{\Omega}_j \\ &= 2 \cdot \mathbf{\Sigma} + \mathbf{\Omega}_i + \mathbf{\Omega}_j,\end{aligned} \tag{14}$$

and the objective function thus becomes

$$T_{ij}(\mathbf{\xi}) = \sum_{l=1}^{n_{sp}} \Delta \hat{\mathbf{y}}_{ij}(\mathbf{\xi}, t_l)' \cdot \mathbf{\Psi}_{ij}(\mathbf{\xi}, t_l)^{-1} \cdot \Delta \hat{\mathbf{y}}_{ij}(\mathbf{\xi}, t_l). \tag{15}$$

The objective functions described above were developed to discriminate between two models. To discriminate between more than two rival models, two approaches can be followed. In a first approach [14,41], an optimal discriminatory experiment is designed for each model pair. When $m$ models are proposed, this means that $\frac{m!}{(m-2)! \cdot 2!}$ experiments have to be designed. From these experiments, the one associated with the highest $T_{ij}(\mathbf{\xi})$ value will eventually be performed. In this way, it should be possible to eliminate the worst models faster compared to the alternative approach [41,12,20], where the optimal discriminatory experiment is designed as follows

$$\mathbf{\xi}^{\star} = \arg \max_{\mathbf{\xi} \in \Xi} \sum_{i=1}^{m-1} \sum_{j=i+1}^{m} T_{ij}(\mathbf{\xi}). \tag{16}$$

In this approach, the value of the objective function can be seen as a measure of the average discriminatory potential over all model pairs. This approach requires less computational resources, but may lead to an experiment where the discriminatory potential is low for the individual model pairs [41].

### 2.7.2. Anticipatory approach to OED/MD
As advocated above, the objective function proposed by Buzzi-Ferraris and co-workers is superior to the others from a conceptual point of view because of the importance of uncertainty with regard to model discrimination. In addition, others already applied this objective function successfully [10,11,26,41]. The methodology proposed in this paper also uses this objective function, but the methodological framework is modified.

In the Buzzi-Ferraris methodology, the parameter estimation error covariance matrix is estimated from the information present in the experiments that have already been performed, and thus from the corresponding Fisher information matrix (as explained in Section 2.3). This results in the following equation:

$$\Phi^{-1} = \sum_{k=1}^{n_e} \mathbf{FIM}(\mathbf{\xi}_k). \tag{17}$$

In this equation, $n_e$ represents the number of experiments performed prior to the experimental design step, and $\mathbf{FIM}(\mathbf{\xi}_k)$ represents the Fisher information matrix associated with experiment $\mathbf{\xi}_k$. This covariance matrix is used as an input to the experimental design step and is used to estimate the model prediction uncertainties of the new experiment through Eqs. (9), (14) and (15). By doing so, the information that would be gathered when performing the $(n_e+1)$th experiment (and that would eventually be used when the model adequacy is tested) is simply ignored.

In our modified Buzzi-Ferraris methodology, the parameter estimation error covariance matrix is recalculated for each proposed experiment by including the **FIM** associated with it. In this way, the expected information content of the newly designed experiment is accounted for, even before the experiment is performed (anticipatory design). This can be formalized as follows

$$\Phi^{-1} = \sum_{k=1}^{n_e} \mathbf{FIM}(\mathbf{\xi}_k) + \mathbf{FIM}(\mathbf{\xi}_{n_e+1}), \tag{18}$$

where the expected information content of the newly designed experiment is represented by $\mathbf{FIM}(\mathbf{\xi}_{n_e+1})$, and calculated using Eq. (6).

### 2.7.3. Calculation of the objective functions
When designing an optimal discriminatory experiment, the optimization algorithm (see Section 2.8) will propose an experiment which is evaluated after calculating the value of the objective function ($T_{ij}$). For the objective functions given by Eqs. (11) and (13), the calculation of $T_{ij}$ is straightforward.

However, the calculation of the other objective function, that is Eq. (15), is more complicated, and it may not be easy to extract the different steps that have to be performed from the equations. Therefore, the different steps are depicted in Fig. 3 and will be described below.

As stated in the previous section, this objective function (Eq. (15)) is used by both the Buzzi-Ferraris and the modified Buzzi-Ferraris methodology. The full-line boxes in Fig. 3 represent the different steps performed when designing an optimal discriminatory experiment according to the Buzzi-Ferraris methodology, while the dashed-line boxes represent the additional steps to be performed when applying the modified Buzzi-Ferraris methodology proposed in this work (anticipatory approach). The original Buzzi-Ferraris methodology starts from an estimate of the parameter estimation error covariance matrix, which is calculated prior to the experimental design step (from Eqs. (17) and (5)) and remains the same throughout the experimental design. In the anticipatory approach, the parameter estimation error covariance matrix is recalculated for each proposed experiment (using Eq. (18)), and is then used in the calculation of $T_{ij}$ through Eqs. (9), (14) and (15).

### 2.8. Optimization algorithms

Both parameter estimation and optimal experimental design are optimization problems. To find the optimum, the use of an optimization algorithm is required. In this work, the SIMPSA optimization algorithm proposed by Cardoso et al. [15] was used. This algorithm combines the non-linear simplex [36] and the simulated annealing
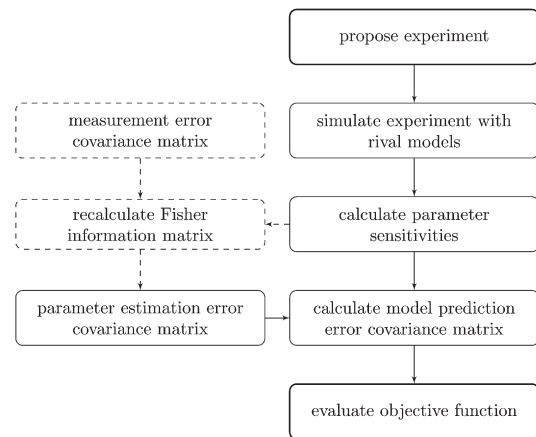


Fig. 3. The full-line boxes (–) in this figure represent the different steps currently performed when designing an optimal discriminatory experiment according to the Buzzi-Ferraris methodology. In the modified Buzzi-Ferraris methodology a number of additional steps are performed, which are shown by the dashed-line boxes (– –).

algorithm [25], and it showed good performance for both the parameter estimation and the experimental design problems encountered in this work. For more information on these optimization algorithms, the reader is referred to the cited papers.

The SIMPSA algorithm was selected from the many different optimization algorithms described in literature (for instance, in [6,7,31,32]) for two reasons. First, because it is a global optimization algorithm. This is important because both parameter estimation experimental design problems can suffer from local minima/maxima, and the use of a global optimization algorithm is therefore required. Several examples can be found in literature where such algorithms were used, both for parameter estimation [16,32,39] and experimental design exercises [5,19,32,43]. Second, because it requires little to no configuration. Typically, several parameters are available to tune an algorithm, and the values at which they are set determine the efficiency of the optimization algorithm. However, the optimal settings are mostly problem specific, and manual tuning is typically required. With the SIMPSA algorithm, some of the parameters are automatically tuned and the number of parameters that remains to be tuned manually is limited.

To handle constraints on the optimization variables, which can be parameters and experimental degrees of freedom in this context, a penalty function was used. When the optimization algorithm proposed a value lying beyond the upper or lower bound, the corresponding value of the objective function was decreased (maximization) or increased (minimization) with a large penalty term that increased as the proposed value was further away from the bound.

### 2.9. Notations for the different approaches

Given the theoretical aspects outlined in Sections 2.7.1 and 2.7.2, four possible approaches can be followed to design an optimal discriminatory experiment. Here, a notation is introduced that should simplify the discussion of the case study presented in Section 3.

The notations $T_a$ and $T_b$ will respectively be used to indicate the approaches in which the objective functions given by Eqs. (11) and (13) are used. The Buzzi-Ferraris methodology and the modified Buzzi-Ferraris methodology will be referred to as $T_c$ and $T_d$, respectively.

## 3. Results and discussion

In this section, the general methodology (as depicted in Fig. 1) and the experimental design concepts introduced in the previous section in particular, will be illustrated on a relatively simple example, where two models are proposed to describe the *in vitro* kinetics of the enzyme glucokinase (*glk*, EC: 2.7.1.2). This enzyme catalyzes the conversion of glucose (GLU) and ATP to glucose-6-phosphate (G6P) and ADP, which is the first reaction of the glycolysis pathway.

### 3.1. General model

Before describing the different kinetics, a general model for the enzymatic conversion process is formulated. For this, it is assumed that the experimental setup allows one to give a pulse of glucose, ATP and PEP, or a mixture thereof.

The volume of the reaction vessel [L], denoted as V, is determined by the flow rate of the pulse [L/s], denoted as $F_p$, and by the sampling (frequency and volume). However, in this example, the sampling volume will be neglected and the volume can thus be described by

$$\frac{dV}{dt} = F_p. \tag{19}$$

For the concentration of glucokinase [mg/L], denoted as GLK, only a dilution effect is considered. Inactivation of the enzyme is neglected,

which is a reasonable assumption since a typical experiment ends after 20 min. The resulting equation for describing the enzyme concentration is given as

$$\frac{dGLK}{dt} = -\frac{F_p}{V} \cdot GLK. \tag{20}$$

The equations used to describe the other state variables (all of which are expressed in mM) are given as:

$$\frac{dGLU}{dt} = \frac{F_p}{V} \cdot (GLU_p - GLU) - v_{glk}, \tag{21}$$

$$\frac{dATP}{dt} = \frac{F_p}{V} \cdot (ATP_p - ATP) - v_{glk}, \tag{22}$$

$$\frac{dG6P}{dt} = -\frac{F_p}{V} \cdot G6P + v_{glk}, \tag{23}$$

$$\frac{dADP}{dt} = -\frac{F_p}{V} \cdot ADP + v_{glk}, \tag{24}$$

$$\frac{dPEP}{dt} = \frac{F_p}{V} \cdot (PEP_p - PEP). \tag{25}$$

Here, $GLU_p$, $ATP_p$ and $PEP_p$ represent the concentrations [mM] of glucose, ATP and PEP in the pulse, respectively, and $v_{glk}$ represents the velocity equation describing the kinetic behavior of glucokinase [mM/s].

As stated before, the kinetic equation is different for the two rival models. However, each one is of the following form:

$$v_{glk} = k \cdot GLK \cdot \frac{\frac{GLU}{K_{GLU}} \cdot \frac{ATP}{K_{ATP}}}{\varphi(GLU, ATP, PEP)}, \tag{26}$$

where the parameter $k$ expresses the maximum specific reaction rate [U/mg], where one unit is defined as that amount of enzyme that catalyzes 1 μmol of substrate in 1 min. The part that is different for the rival models is represented by $\varphi(GLU, ATP, PEP)$.

### 3.2. Rival models

The conversion catalyzed by glucokinase is a bi-reactant system [42]. Two reaction mechanisms are possible for such a system: random and ordered. In a random bi-reactant system the order in which the two substrates bind doesn't matter, whereas in an ordered bi-reactant system one of the substrates has to bind to the enzyme first, before the second substrate can bind and the reaction can take place. In addition, it was recently suggested that glucokinase may be inhibited by phosphoenolpyruvate (PEP) [37], and more specifically that PEP inhibits the binding of ATP to the enzyme.

Based on these considerations, two models were built to describe the enzyme kinetics. The models differ in the equation used to describe the enzyme kinetics, each of which is based on a particular hypothesis of how the enzyme works (random or ordered bi-reactant system).

For model $m_1$, it was assumed that the reaction mechanism of glucokinase was a random bi-reactant system. Since PEP inhibited the binding of ATP to the enzyme, this results in the following equation:

$$\varphi(GLU, ATP, PEP) = 1 + \frac{GLU}{K_{GLU}} + \frac{ATP}{K_{ATP}} + \frac{PEP}{K_{PEP}} + \frac{GLU}{K_{GLU}} \cdot \frac{PEP}{K_{PEP}} + \frac{GLU}{K_{GLU}} \cdot \frac{ATP}{K_{ATP}}. \tag{27}$$

For model $m_2$, an ordered reaction mechanism was assumed, which results in the following equation:

$$\varphi(\text{GLU}, \text{ATP}, \text{PEP}) = 1 + \frac{\text{GLU}}{K_{\text{GLU}}} + \frac{\text{GLU}}{K_{\text{GLU}}} \cdot \frac{\text{PEP}}{K_{\text{PEP}}} + \frac{\text{GLU}}{K_{\text{GLU}}} \cdot \frac{\text{ATP}}{K_{\text{ATP}}}.$$  (28)

### 3.3. Real model and data generation

According to literature [33,37], the reaction mechanism of glucokinase is ordered, with glucose as the first binding substrate, and PEP inhibits the binding of ATP to the enzyme. Based on these considerations, the second model was chosen as the real model ($m_2^\star$). This model was used to generate experimental data by simulating the experiment using the parameter values tabulated in Table 1, and by adding random noise to mimic the measurement error. The standard deviations of the measurements were calculated in the same way as suggested by Ternbach [43]:

$$\sigma_y = \hat{y} \cdot \varsigma_y \cdot \left( 1 + \frac{1}{\frac{\hat{y}}{\text{lb}_y} + \left(\frac{\hat{y}}{\text{lb}_y}\right)^2} \right).$$  (29)

Here, $\varsigma_y$ represents a constant minimal relative error, and $\text{lb}_y$ represents the lower accuracy bound on the measurement of $y$. In this way, the standard deviation of the measurements are proportional to the value of $\hat{y}$, but increase when the latter approaches the lower accuracy bound on the measurement.

### 3.4. Preliminary experiment

To initiate the case study, a preliminary experiment was defined and performed in silico. For this experiment, the volume of the reaction vessel was set to 10 mL, and the initial glucokinase concentration was set such that 5 units were present in the reaction mixture. Further, it was assumed that no G6P, ADP and PEP were present at the start of the experiment, and the initial concentrations of glucose and ATP were set to 1.5 mM and 0.5 mM, respectively.

During the experiment, two pulses were given, with the pulse volume of to 1 mL. The first pulse was given 5 min after the start of the experiment, and contained only ATP. The ATP concentration in the pulse was chosen such that the ATP concentration in the reaction mixture was raised to 1.5 mM. The second pulse, given 10 min after the start of the experiment, contained glucose and PEP, and their concentrations in the pulse were chosen such that the resulting concentrations in the reaction mixture were 1.5 mM and 0.1 mM, respectively.

The experiment stopped after 20 min, and ten measurements of glucose, ATP, G6P and ADP were taken in duplicate (see Fig. 4). The minimal relative errors ($\varsigma$) were set to 0.05 for all measured state variables, and the lower accuracy bounds on the measurements were defined as 0.1 mM.

### 3.5. Parameter estimation

The parameters of the rival models were estimated using the data from the preliminary experiment (Fig. 4), and using the optimization algorithm described in Section 2.8. Since negative parameter values would not make any sense, the lower bounds were set to zero. The upper bounds were set to 1000 U/mg for parameter $k$, 2 mM for parameter $K_{\text{GLU}}$, and 25 mM for both parameters $K_{\text{ATP}}$ and $K_{\text{PEP}}$.

The results of this parameter estimation exercise are shown in Table 1, and Fig. 5 shows how both models describe the experimental data after estimating their parameters. The figure also shows the 95% confidence intervals on these model predictions, which represent the uncertainty associated with them. One can see that these confidence intervals sometimes become negative, which is of course unrealistic and is due to the fact that the model prediction uncertainties were obtained by linearly propagating the uncertainty on the parameter estimates.

### 3.6. Model adequacy testing

The good agreement between the data and the model predictions is obviously reflected in a relatively small value of the sum of squared errors (SSE). As shown in Table 1, the SSE-values for models $m_1$ and $m_2$ were 57.1080 and 56.9285, respectively. According to the model adequacy test outlined in Section 2.6, these values have to be compared to the critical $\chi^2$ value taken from a $\chi^2_{76}$ distribution ($n=80$ and $n_p=4$) with a chosen confidence level of 95%, which is equal to 97.3510. From this, one can conclude that both models adequately describe the data.

### 3.7. Design of optimal discriminatory experiments

Since both models passed the model adequacy test, an experiment should be designed to discriminate between them. In order to make the differences between the approaches easier to explain and interpret, the experimental design was restricted to only optimizing the measurement times, while keeping the other experimental degrees of freedom fixed. In addition, this restriction led to a drastic decrease of required computation time, as will be discussed in Section 3.11.

For this experimental design exercise, a new experiment was defined and the optimal sampling times were determined using the different approaches ($T_a$, $T_b$, $T_c$ and $T_d$). In this experiment, three pulses were given, for each of which the volume was equal to 1 mL. The first pulse was given 5 min after the start of the experiment, and contained ATP and PEP. The ATP concentration in the pulse was chosen such that the ATP concentration in the reaction mixture was raised to 1.5 mM. The concentration of PEP in the pulse was set to 0.5 mM, which was also the case for the other pulses. The second pulse, given 10 min after the start of the experiment, contained glucose and PEP, and the glucose concentration was chosen such that the resulting concentration was 1.5 mM. The third pulse contained ATP and PEP, and the concentration of the former was set to 3 mM. The experiment stopped after 20 min, and only glucose and ADP were measured. These measurements were taken in duplicate, and the minimal relative errors ($\varsigma$) were set to 0.015 for the measured state variables, and the lower accuracy bounds on the measurements were defined as 0.1 mM. Further, the minimum time interval between two measurements was set to 15 s.

Using the parameters tabulated in Table 1, the two models predict the experiment as shown in Fig. 5. To gain insight into the different methodologies, ten scenarios were defined with the number of sampling times ranging from one to ten. The results of the scenario in which ten optimal sampling times were determined will be discussed in Section 3.8, and the other scenarios will be discussed in Section 3.9.
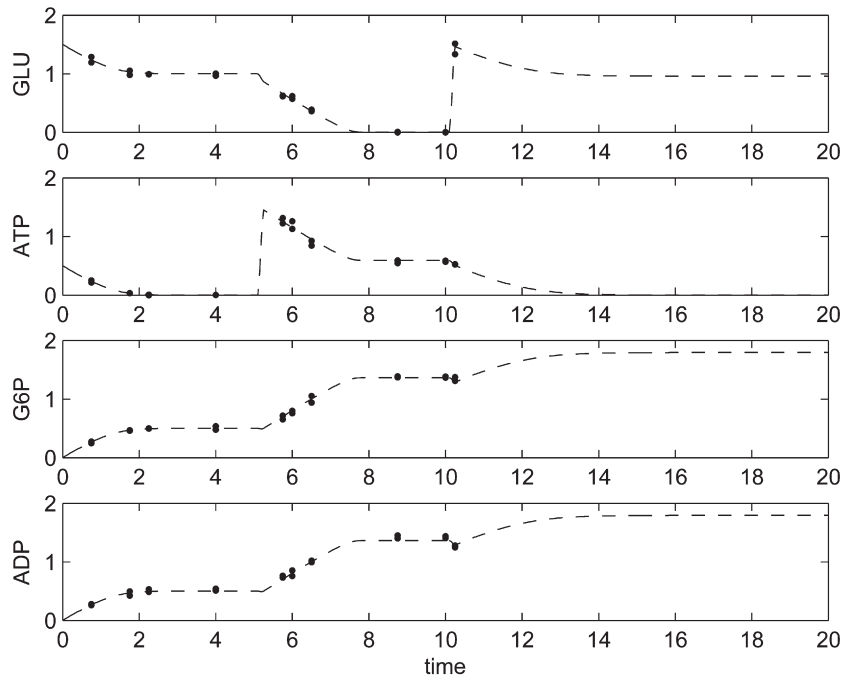
**Table 1**
Parameters of the real model ($m_2^\star$) that were used to generate experimental data, and the parameter estimates obtained after fitting the rival models to the data from the preliminary experiment, together with the corresponding WSSE-values

| Model | $k$ | $K_{\text{GLU}}$ | $K_{\text{ATP}}$ | $K_{\text{PEP}}$ | WSSE |
|---|---|---|---|---|---|
| $m_2^\star$ | 312.00 | 0.1500 | 0.1300 | 0.1000 | – |
| $m_1$ | 308.05 | 0.0087 | 0.1390 | 2.8963 | 57.1080 |
| $m_2$ | 309.81 | 0.2429 | 0.1152 | 0.0276 | 56.9285 |

**Fig. 4.** Simulation of the preliminary experiment (– –) using the real model ($m_2^\star$), as well as the experimental data (●) obtained from it.

### 3.8. Discussion of the experiment with ten samples

The results of the scenario in which ten optimal sampling times were determined are shown in Fig. 7. For each of the presented approaches ($T_a$, $T_b$, $T_c$ and $T_d$), the discriminatory power at a given point in time can be calculated using the appropriate objective function (Eqs. (11), (13) or (15)), by assuming that one only samples at that time. The trajectories of the objective functions obtained in this way are shown in Fig. 7, as well as the optimal sampling times obtained from them.

The upper graph of Fig. 7 shows the trajectory of the objective function used in the $T_a$ approach. This objective function (calculated using Eq. (11)) represents the difference in the model predictions. From the graph, one can see that the difference between the models is rather small, with the biggest difference occurring around 12 min. So, the optimal sampling times are predominantly located in this region when only the model predictions are considered ($T_a$ approach).

The second graph of Fig. 7 shows the trajectory of the objective function used in the $T_b$ approach, which differs from the $T_a$ approach
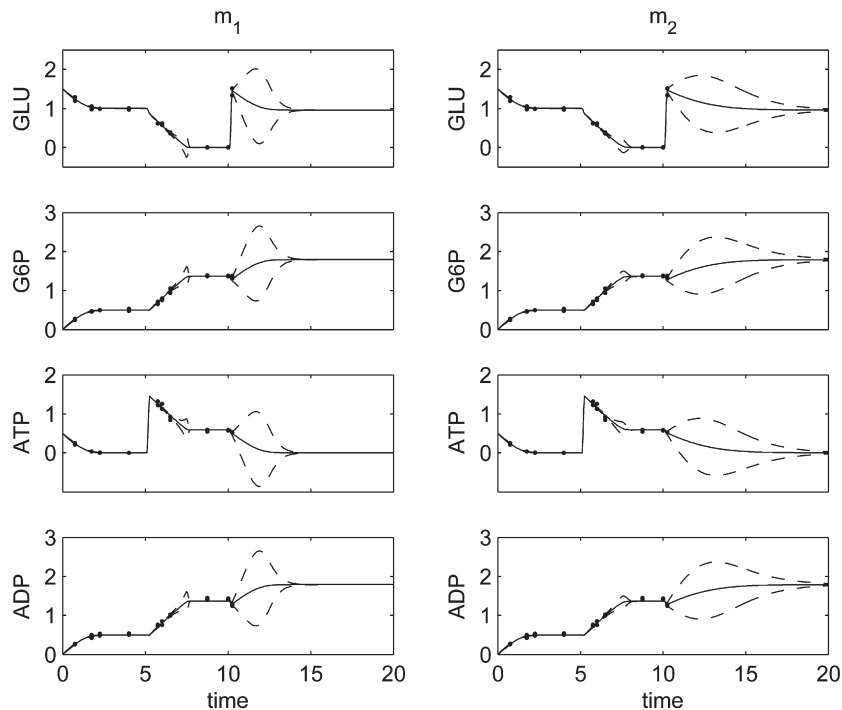


**Fig. 5.** Rival models predicting (—) the data from the preliminary experiment (●) after parameter estimation, as well as the 95% confidence intervals on the model predictions (– –).
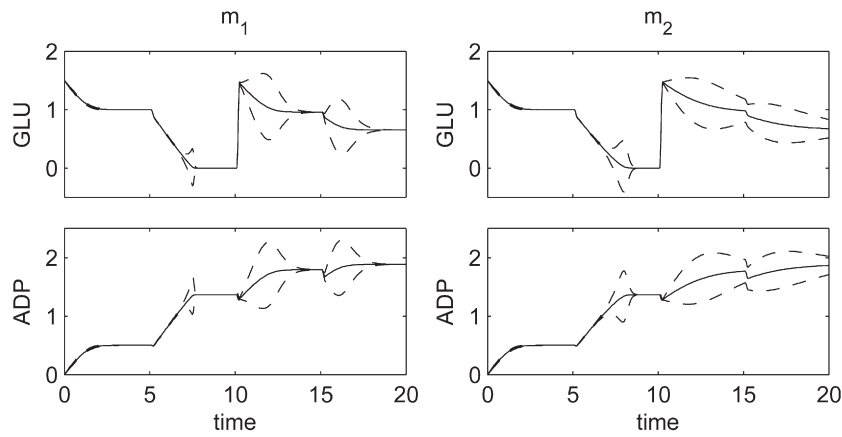
**Fig. 6.** Rival models predicting (—) the experiment for which the sampling times were optimized. The dashed lines represent the 95% confidence intervals on the model predictions.

by the fact that the measurement uncertainty is accounted for. The latter is more or less proportional to the values of the measured state variables (see Eq. (29)), which explains the obtained results. Indeed, from Figs. 6 and 7, one can see that the largest difference in the model prediction occurs at relatively high values of the measured state variables, which are thus associated with relatively high measurements errors. The optimal sampling times are therefore partly shifted to the regions around 7 min and 17 min, where the measurement errors are smaller.

In the $T_c$ approach, the model prediction uncertainties (shown in Fig. 5) are taken into account. These uncertainties are quite high, especially where a large difference between the model predictions is observed. This results in very low values of the objective function (Eq. (15)), and thus in a low discriminatory power of the experiment. In fact, the value of $T_{ij}$, which is obtained as the sum of the values of the individual sampling times, is merely equal to 1.14. According to Chen et al. [17], the experiment is worth performing when this value is larger than $n_{sp} \cdot n_m$, which is 20 in our example (two measured state variables and ten sampling times).

When applying the anticipatory approach ($T_d$ approach), the parameter and model prediction uncertainties are recalculated for each experiment the optimization algorithm proposes. The optimal sampling times that were obtained in this way, are spread out over the three regions where the difference in the model predictions is significant (see Fig. 7). The model prediction uncertainties associated with this optimal experiment, which were also used when calculating the objective function (Eq. (15)), are shown in Fig. 8. As can be seen, it was possible to significantly reduce the model prediction uncertainty, and an experiment is obtained that resembles the one found with the $T_b$ approach.

### 3.9. Apparent similarity between $T_b$ and $T_d$

As discussed in the previous section, the $T_d$ approach seemed to bring forth a similar experiment as the one obtained by the $T_b$ approach, although the latter does not consider the uncertainty on the model predictions. The reason why both approaches result in a similar experiment is that the information content of the designed experiment
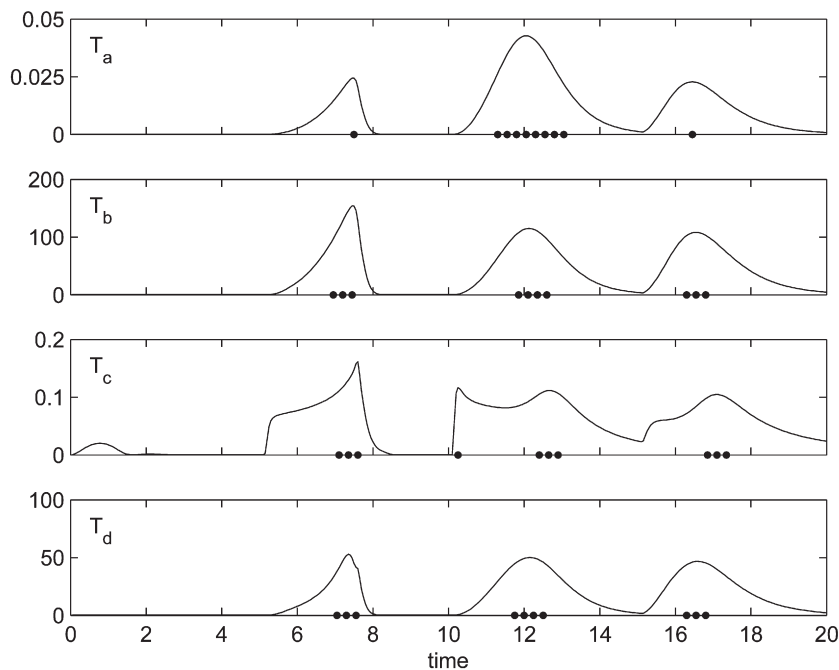


**Fig. 7.** From top to bottom, these graphs show the trajectory of the objective function obtained when, respectively, the approaches $T_a$, $T_b$, $T_c$ and $T_d$ were applied to determine the optimal sampling times (●) in the scenario with ten samples.
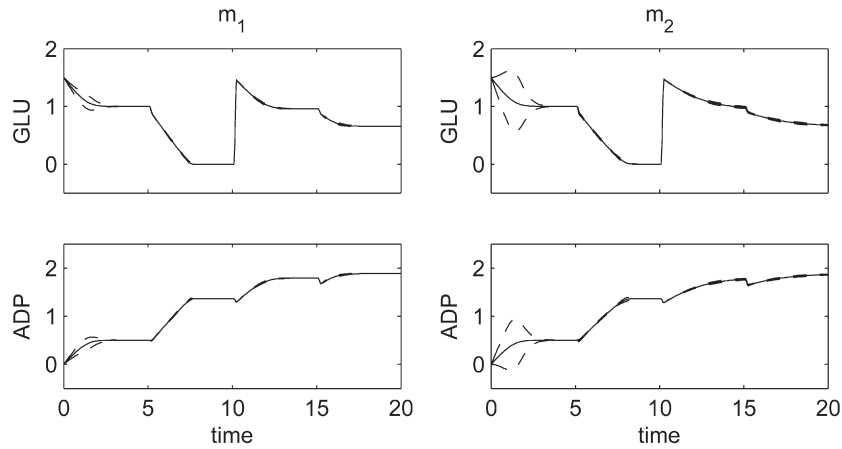
**Fig. 8.** Rival models predicting (—) the experiment for which the sampling times were optimized. The dashed lines (– –) represent the 95% confidence intervals on the model predictions as they were used when applying the anticipatory approach.

is large enough to decrease the prediction uncertainty to a level where its impact on the experimental design becomes rather limited. To investigate this similarity in more detail, nine additional experimental design exercises were performed, where the number of samples to be optimized ranged from one to nine. The results are shown in Fig. 9 as well as those from the scenario with ten samples.

One clearly sees that the similarity between the experiments designed using the $T_b$ and the $T_d$ approach does not always exist. In fact, some interesting observations can be made from Fig. 9 that clearly illustrate the anticipatory nature and the power of the $T_d$ approach. For instance, when one or two samples are optimized, the region with the largest difference in the model predictions (around 12 min) cannot be exploited because the uncertainty in this region cannot be sufficiently reduced. However, with three and more samples, this is no longer the case. In addition, three samples appear to be enough, since the fourth, fifth and sixth samples to reduce the uncertainty in the region around 17 min. Another example is found when comparing the scenarios with seven, eight and nine samples.

These show that it appears to be beneficial to place the eighth sample in the region around 12 min, rather than placing it in the region around 7 min. However, when nine samples are optimized, two samples are placed in this region. Apparently, one point cannot achieve a sufficient decrease in model prediction uncertainty, while two samples can.

From the discussion above, it is clear that the $T_b$ and the $T_d$ approaches do not always lead to the same experiments. In fact, this is only the case when the information content of the designed experiment is high enough to reduce the model prediction uncertainty beyond a certain level. If that is the case, the impact of $\Omega_i$ and $\Omega_j$ from Eq. (14) will become so small, that the experimental design will be dominated by the measurement error ($\Sigma$), and thus a similar experiment will be found as with the $T_b$ approach.

It is of course impossible to foresee this, and one cannot know beforehand whether the experiments designed using these approaches will be similar or not. The premise that both approaches lead to similar experiments is thus not a valid one.
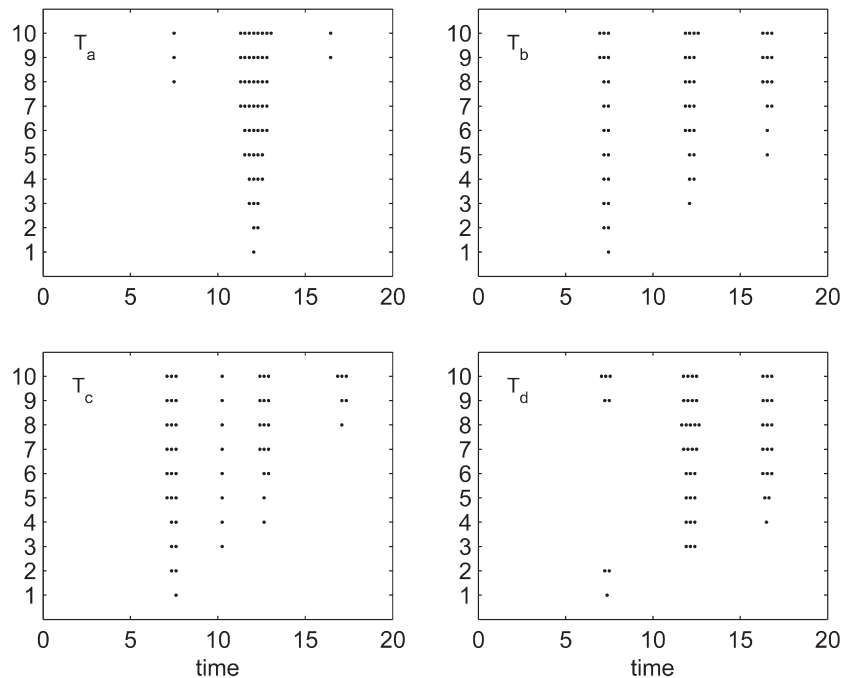


**Fig. 9.** Optimal sampling times obtained after applying the $T_a$, $T_b$, $T_c$ and $T_d$ approaches for the ten different scenarios in which the number of sampling times ranges from one to ten.

*3.10. A note on the estimate of the uncertainty on the model predictions*

As advocated in Section 2.7.1, the uncertainty on the model predictions is important with regard to model discrimination, and more specifically for the design of discriminatory experiments. In principle, both the $T_c$ and the $T_d$ approach will select the experimental degrees of freedom such that the expected model prediction uncertainty is small at the times when samples are taken, thereby increasing the discriminatory potential of the resulting experiment. However, the anticipatory nature of the $T_d$ approach is likely to result in more reliable estimates of the model prediction uncertainties that will eventually obtained after performing the designed experiment and re-estimating the model parameters.

This is illustrated in Fig. 10. Here, the uncertainties on the model predictions of glucose are shown (the results for ADP are similar). For clarity, these are the values that are added to/subtracted from the model predictions to get figures like Figs. 6 and 8. Fig. 10 compares the model prediction uncertainties as they are used in the $T_c$ approach (dashed lines in the upper graphs) and in the $T_d$ approach (dashed lines in the lower graphs) to those obtained after the experiment is performed and the model parameters were re-estimated (dotted lines). From this figure, one can clearly see that the model prediction uncertainties used in the experimental design (dashed lines) are closer to the dotted lines when the $T_d$ approach was used.

Note that the model adequacy test described in Section 2.6 does not consider the model prediction uncertainty. In fact, little attention has been given to this aspect in literature so far. Nevertheless, the anticipatory approach proposed in this paper provides a way to accommodate for this.

*3.11. Computational costs of the different approaches*

In the search for the optimal discriminatory experiment, many experiments are proposed by the optimization algorithm for which the discriminatory potential has to be assessed. The latter requires some prior calculations of which the computational costs differ for the presented approaches.

In the $T_a$ approach, simulating the experiment with the rival models brings forth all information necessary to calculate the trajectory of the objective function. When the $T_b$ approach is applied, the measurement uncertainties are necessary as well. Although these were calculated from the simulation results in this *in silico* example, they are not calculated in practical applications but determined by the experimental setup. Hence, the computational costs associated with the $T_a$ and $T_b$ approaches are identical.

When the parameter and model prediction uncertainty have to be estimated, which is the case for the $T_c$ and $T_d$ approaches, the model is extended with additional ordinary differential equations to calculate the parameter sensitivities. This will obviously result in a larger computational cost. The additional computational cost caused by the fact that the parameter estimation error covariance matrix has to be recalculated in the $T_d$ approach is minor and only involves some extra matrix manipulations, as can be concluded from Eqs. (5) and (18).

Note that in the special case where only the measurement times are to be optimized (as in the case study presented in this paper), the use of an optimization algorithm is not necessary for the $T_a$, $T_b$ and $T_c$ approaches. This is because the choice of the sampling times has no effect on the model predictions, nor on the model prediction uncertainties. In other words, the trajectory of $T_{ij}$ is calculated once, and the optimal sampling times are easily determined from this trajectory. For the $T_d$ approach, this is not the case, and a new trajectory of $T_{ij}$ has to be calculated for each set of the sampling times. However, the extra computational costs are relatively small, because the values of the parameter sensitivities at the proposed sampling times can be obtained by sampling from the (detailed) parameter sensitivity profiles calculated prior to the experimental design exercise.

## 4. Conclusions

This paper dealt with experimental design methodologies that are used to find the experimental conditions that allow to discriminate among rival models with the least experimental effort. For this, the expected experimental results should be predicted differently by the rival models, and the uncertainty on the measurements and on the model predictions should not be too large. In this paper, three existing approaches to deal with the problem of model discrimination were described, one of which (the one developed by Buzzi-Ferraris and co-workers in 1984 [13]) was improved by taking into the expected information content of the newly designed experiment, even before the experiment is performed (anticipatory design).

The presented approaches were illustrated and compared by applying them to a case study in which two rival models were proposed to describe the kinetics of an enzyme. The experimental design exercise consisted of determining the optimal sampling times for a given dynamic profile of the manipulatory variables. The results showed that the anticipatory approach arranges the experimental degrees of freedom such that the expected model prediction uncertainty is small at the times when samples are taken, thereby increasing the discriminatory potential of the resulting experiment.
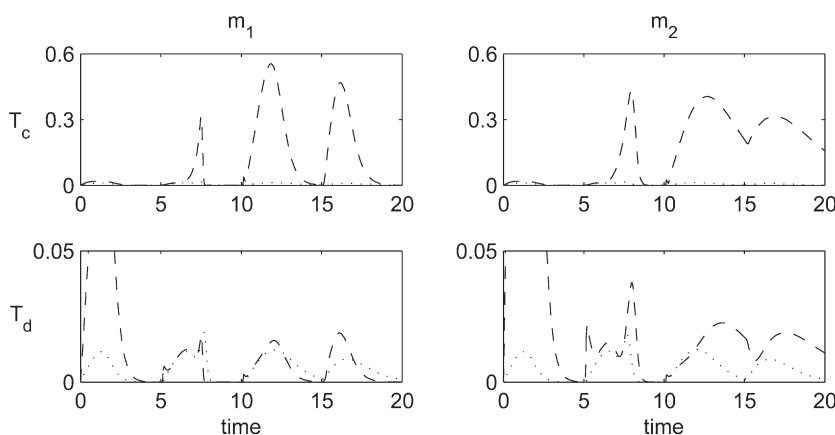


**Fig. 10.** The 95% confidence intervals associated with the model predictions of the glucose concentration as used when designing an experiment according to the $T_c$ approach (dashed lines in the upper graphs), and according to the $T_d$ approach (dashed lines in the lower graphs), as well as the ones obtained after performing the designed experiment and after re-estimating the parameters (dotted lines).

The results also showed that applying the anticipatory approach can result in an experiment that is similar to the one found with the simpler and less computationally expensive approach that only includes the uncertainty on the measurements. This was the case when the information content of the designed experiment was large enough to decrease the model prediction uncertainty to a level where its impact on the experimental design was rather limited, and the experimental design became dominated by the measurement error.

In addition, the results showed that, compared to the original approach, the anticipatory approach led to more reliable estimates of the model prediction uncertainties that are eventually obtained after performing the designed experiment and re-estimating the model parameters. This is important because when this estimate is far from the one eventually used in the model adequacy test, the discriminatory potential of the experiment may not be as high as expected while designing the experiment.

## Acknowledgments

## References

[1] S.P. Asprey, S. Macchietto, Statistical tools for optimal dynamic model building, Computers and Chemical Engineering (2000) 1261–1267.
[2] S.P. Asprey, S. Macchietto, Designing robust optimal dynamic experiments, Journal of Process Control (2002) 545–556.
[3] A.C. Atkinson, A.N. Donev, Optimum Experimental Design, Oxford University Press, New York, 1992 328 pages.
[4] M. Baltes, R. Schneider, C. Sturm, M. Reuss, Optimal experimental design for parameter estimation in unstructured growth models, Biotechnology Progress (1994) 480–488.
[5] J.R. Banga, K.J. Versyck, J.F. Van Impe, Computation of optimal identification experiments for nonlinear dynamic process models: a stochastic global optimization approach, Industrial and Engineering Chemistry Research (2002) 2425–2430.
[6] J.R. Banga, C.G. Moles, A.A. Alonso, Global optimization of bioprocesses using stochastic and hybrid methods, Frontiers in Global Optimization — Nonconvex Optimization and its Applications, vol. 74, Kluwer Academic Publishers, 2003, 597 pages.
[7] J.R. Banga, E. Balsa-Canto, C.G. Moles, A.A. Alonso, Dynamic optimization of bioprocesses: efficient and robust numerical strategies, Journal of Biotechnology (2005) 407–419.
[8] L. Benabbas, S.P. Asprey, S. Macchietto, Curvature-based methods for designing optimally informative experiments in multiresponse nonlinear dynamic situations, Industrial and Engineering Chemistry Research (2005) 7120–7131.
[9] K. Bernaerts, K.J. Versyck, J.F. Van Impe, On the design of optimal dynamic experiments for parameter estimation of a Ratkowsky-type growth kinetics at suboptimal temperatures, International Journal of Food Microbiology (2000) 27–38.
[10] A.L. Burke, T.A. Duever, A. Penlidis, Model discrimination via designed experiments: discrimination between the terminal and penultimate models based on rate data, Chemical Engineering Science 10 (1995) 1619–1634.
[11] A.L. Burke, T.A. Duever, A. Penlidis, An experimental verification of statistical discrimination between the terminal and penultimate polymerization models, Journal of Polymer Science: Part A: Polymer Chemistry (1996) 2665–2678.
[12] A.L. Burke, T.A. Duever, A. Penlidis, Discriminating between the terminal and penultimate models using designed experiments: an overview, Industrial and Engineering Chemistry Research (1997) 1016–1035.
[13] G. Buzzi-Ferraris, P. Forzatti, G. Emig, H. Hofmann, Sequential experimental design procedure for model discrimination in the case of multiple responses, Chemical Engineering Science 1 (1984) 81–85.
[14] G. Buzzi-Ferraris, P. Forzatti, P. Canu, An improved version of a sequential design criterion for discriminating among rival multiresponse models, Chemical Engineering Science 2 (1990) 477–481.
[15] M.F. Cardoso, R.L. Salcedo, S. Feyo de Azevedo, The simplex-simulated annealing approach to continuous non-linear optimization, Computers and Chemical Engineering 9 (1996) 1065–1080.
[16] N. Checchi, S. Marsili-Libelli, Reliability of parameter estimation in respirometric models, Water Research, (2005) 3686–3696.
[17] B.H. Chen, S.P. Asprey, On the design of optimally informative dynamic experiments for model discrimination in multiresponse nonlinear situations, Industrial and Engineering Chemistry Research, (2003) 1379–1390.
[18] A. de Brauwere, F. De Ridder, R. Pintelon, M. Elskens, J. Schoukens, W. Baeyens, Model selection through a statistical analysis of the minimum of a weighted least squares cost function, Chemometrics and Intelligent Laboratory Systems, (2004) 163–173.
[19] D.J.W. De Pauw, P.A. Vanrolleghem, Designing and performing experiments for model calibration using an automated iterative procedure, Water Science and Technology 1 (2006) 117–127.
[20] F.J. Dumez, The use of sequential discrimination in the study of 1-butane dehydrogenation, Industrial and Engineering Chemistry Fundamentals 2 (1977) 298–301.
[21] D. Espie, S. Macchietto, The optimal design of dynamic experiments, American Institute of Chemical Engineers, AIChE Journal 2 (1989) 223–229.
[22] G.C. Goodwin, R.L. Payne, Dynamic System Identification: Experiment Design and Data Analysis, Academic Press, New York, 1977 299 pages.
[23] W.G. Hunter, A.M. Reiner, Designs for discriminating between two rival models, Technometrics, (1965) 307–323.
[24] M. Joshi, A. Seidel-Morgenstern, A. Kremling, Exploiting the bootstrap method for quantifying parameter confidence intervals in dynamical systems, Metabolic Engineering, (2006) 447–455.
[25] S. Kirkpatrick, C.D. Gelatt, M.P. Vecchi, Optimization by simulated annealing, Science, (1983) 671–680.
[26] A. Kremling, S. Fischer, K. Gadkar, F.J. Doyle, T. Sauter, E. Bullinger, F. Allgöwer, E.D. Gilles, A benchmark for methods in reverse engineering and model discrimination: problem formulation and solutions, Genome Research (2004) 1773–1785.
[27] J.R. Leis, M.A. Kramer, The simultaneous solution and sensitivity analysis of systems described by ordinary differential equations, ACM Transactions on Mathematical Software 1 (1988) 45–60.
[28] L. Ljung, System Identification, Theory for the user, Prentice Hall, 1999 608 pages.
[29] S. Marsili-Libelli, S. Guerrizio, N. Checchi, Confidence regions of estimated parameters for ecological systems, Ecological Modelling (2003) 127–146.
[30] R. Mehra, Optimal input signals for parameter estimation in dynamic systems — survey and new results, IEEE Transactions on Automatic Control 6 (1974) 753–768.
[31] P. Mendes, D.B. Kell, Non-linear optimization of biochemical pathways: applications to metabolic engineering and parameter estimation, Bioinformatics 10 (1998) 869–883.
[32] C.G. Moles, P. Mendes, J.R. Banga, Parameter estimation in biochemical pathways: a comparison of global optimization methods, Genome Research (2003) 2467–2475.
[33] O. Monasterio, M.L. Cárdenas, Kinetic studies of rat liver hexokinase D ('glucokinase') in non-co-operative conditions showing an ordered mechanism with MgADP as the last product to be released, Biochemical Journal (2003) 29–38.
[34] A. Munack, Optimal Feeding Strategy for Identification of Monod-type Models by Fed-batch Experiments, in: N.M. Fish (Ed.), Computer Applications in Fermentation Technology: Modelling and Control of Biotechnological Processes, 4th ed., SCI Elsevier Applied Science Publishing, Amsterdam, 1989, pp. 195–204.
[35] A. Munack, Optimization of Sampling, in: K. Schügerl (Ed.), Biotechnology, a Multi-volume Comprehensive Treatise, Measuring, Modelling and Control, vol. 4, VCH, Weinheim, 1991, pp. 251–264.
[36] J.A. Nelder, R. Mead, A simplex method for function minimization, Computer Journal, (1965) 308–313.
[37] T. Ogawa, H. Mori, M. Tomita, M. Yoshino, Inhibitory effect of phosphoenolpyruvate on glycolytic enzymes in Escherichia coli, Research in Microbiology, (2007) 159–163.
[38] M. Omlin, P. Reichert, A comparison of techniques for the estimation of model prediction uncertainty, Ecological Modelling 1 (1999) 45–49.
[39] M. Rodriguez-Fernandez, P. Mendes, J.R. Banga, A hybrid approach for efficient and robust parameter estimation in biochemical pathways, Biosystems 2–3 (2006) 248–265.
[40] R.W. Shirt, T.J. Harris, D.W. Bacon, Experimental design considerations for dynamic systems, Industrial and Engineering Chemistry Research, (1994) 2656–2667.
[41] M. Schwaab, F.M. Silva, C.A. Queipo, A.G. Barreto Jr., M. Nele, J.C. Pinto, A new approach for sequential experimental design for model discrimination, Chemical Engineering Science, (2006) 5791–5806.
[42] I.H. Segel, Enzyme Kinetics — Behavior and Analysis of Rapid Equilibrium and Steady-state Enzyme Systems, John Wiley & Sons, Inc., 1975 957 pages.
[43] M.A.B. Ternbach, C. Bollman, C. Wandrey, R. Takors, Application of model discriminating experimental design for modeling and development of a fermentative fed-batch L-valine production process, Biotechnology and Bioengineering 3 (2005) 356–368.
[44] P. Vanrolleghem, M. Van Daele, Optimal experimental design for structure characterization of biodegradation models: on-line implementation in a respirographic biosensor, Water Science and Technology 4 (1994) 243–253.
[45] P.A. Vanrolleghem, F. Coen, Optimal design of in-sensor-experiments for on-line modelling of nitrogen removal processes, Water Science and Technology 2 (1995) 149–160.
[46] P.A. Vanrolleghem, D. Dochain, Bioprocess model identification, in: J.F.M. Van Impe, P.A. Vanrolleghem, D.M. Iserentant (Eds.), Advanced Instrumentation, Data Interpretation, and Control of Biotechnological Processes, Kluwer Academic Publishers, 1998, pp. 251–318.
[47] E. Walter, L. Pronzato, Identification of Parametric Models from Experimental Data, Springer-Verlag, Berlin, 1997 413 pages.